Volume 1 | Number 1 | Jan 2013 | Pages 1–100

Journal of
Materials Chemistry A

Materials for energy and sustainability
www.rsc.org/materialsA

ROYAL SOCIETY
OF CHEMISTRY

ROYAL SOCIETY
OF CHEMISTRY

www.rsc.org/materialsA

Responsive Electrolytes that Inhibit Electrochemical Energy Conversion at Elevated Temperatures

Jesse C. Kelly, Rishi Gupta, and Mark E. Roberts*

J. C. Kelly, Prof. M. E. Roberts
Dept. of Chemical & Biomolecular Engineering
Clemson University
204 Earle Hall
Clemson, SC 29634
*E-mail: mrober9@clemson.edu

R. Gupta
Department of Chemical Engineering
University of Virginia
102 Engineers' Way
Charlottesville, VA 22904

Abstract. Energy storage has emerged as a critical challenge due to the increasing demand to utilize energy from intermittent, renewable resources. Furthermore, growing interest in decreasing our dependence on petroleum necessitates the development of safe and efficient energy storage for transportation. Li-ion batteries have emerged as the premier candidate to meet these demands; however, such systems are limited by thermal hazards (runaway reactions, fires, explosions), which become increasingly dangerous in large format batteries. We have developed an electrolyte system comprising poly(ethylene oxide), ionic liquid and lithium salt that exhibits an intrinsic mechanism for inhibiting device operation when the temperature increases beyond a given threshold, which is attributed to polymer-ionic liquid phase separation. In the following article, we describe how the thermally activated phase separation causes a decrease in ion conductivity, thereby affecting the concentration of ions at the electrode, in addition to an increase in charge transfer resistance from the formation of a polymer coating on the porous

electrode. Such mixtures provide a transformative approach to regulating electrochemical processes, which is necessary to achieve an inherently safe operation of large format Li-ion batteries.

1. Introduction

In recent years, room temperature ionic liquids (ILs) have seen increasing interest as potential electrolytes for electromechanical,[1] electrochromic,[2] and dye-sensitized solar cell devices.[3] ILs have also shown promise as electrolyte solvents in future energy storage technologies[4-7] due to their compatibility with various electrode materials and favorable characteristics (negligible volatility, non-flammability, high ionic conductivity, and stability over a wide electrochemical potential range).[8-12] With an increasing demand for improved energy storage systems in portable electronics, transportation and renewable energy generation, research efforts are moving toward developing high power and high energy battery and supercapacitor systems. Lithium ion batteries (LIBs), particularly those capable of high power and high energy operation, show great promise for efficient devices with high power and energy densities. The safety hazards associated with these systems, however, have prevented widespread adaptation and as the need for large-format batteries increases, so does the potential for catastrophic thermal failure.[13]

Common LIB safety issues, such as Li-plating (dendrite formation) and exothermic reactions at the electrode surface, are often associated with conventional electrolytes and eventually lead to short circuits, local overheating, and thermal runaway.[14] Untreated, these issues can result in fires and explosions due to electrolyte volatility and flammability.[15] Efforts to mitigate these issues in commercially available LIBs involve the implementation of solid-state polymer

electrolytes,[16, 17] where low ionic conductivity limits battery performance (particularly the power density), and advanced tri-layer separator materials,[18, 19] where thermal decay occurs at high temperatures rendering the batteries useless. While innovative and continuing to improve,[20, 21] the limitations of these provisional methods will likely not meet the needs for efficient, large-format systems.

Unlike conventional methods that require selection between low-performance devices and destructive safety measures, continuing advances in energy storage will require creative approaches in engineering and material design to mitigate these safety issues. One area of interest is the development of functional LIB electrolytes, particularly doped polymer electrolytes. Poly(ethylene oxide) (PEO) and its derivatives have long been combined with lithium salts to create polymeric electrolytes, which provide a safe, low conductivity alternative to traditional alkyl carbonates and lithium salt mixtures. The performance of these PEO polymer electrolytes, particularly conductivity, has been shown to increase with the addition of traditional molecular solvents; however, these changes reintroduce many of the safety hazards associated with traditional electrolyte materials (electrode/electrolyte reactions, volatility, and flammability). Devices utilizing IL-doped polymers have shown great promise for electrolytes in LIBs without sacrificing on the safety advances that solid polymer electrolytes provide.[22] These systems benefit from the advantageous solvent properties of ILs, which help to increase the PEO mobility, and therefore, conductivity of Li-ions in the PEO/IL mixtures.[23] Even in small compositions, ILs are capable of increasing the conductivity of traditional PEO polymer electrolytes by several orders of magnitude,[24] a necessity for future high power energy storage devices. Additionally, unique combinations of ILs and polymers, including poly(ionic liquids),[25-

[26] polymer and ionic liquid copolymers,[27-28] and solutions of ILs comprising glycol ethers (glymes),[29-30] have shown promise as highly conductive, safe, and reliable electrolytes for advanced electrochemical devices.

Already established in literature as a potential candidate for LIB electrolytes, mixtures of PEO and ILs also exhibit thermally responsive behaviour as a result of their lower critical solution temperature (LCST), which causes the mixture to phase separate above a given temperature.[31-35] Responsive materials are defined based on a macroscopic property that can be manipulated in a specific, reliable, and predictable manner when exposed to an external stimulus or environmental change. [36, 37] Polymers are particularly attractive for responsive systems as their molecular properties can be tailored to add functionality or change the extent to which a desired macroscopic property can be altered.[38] In polymeric materials, the molecular weight, structure, composition and function can be designed to tailor how the materials respond to an external stimulus (e.g. pH, light, temperature, chemical composition, electric or force) and influence a reversible change in the mechanical, electrical, chemical, or optical properties. Due to their demonstrated application in batteries, responsive mixtures of PEO in an IL (1-ethyl-3-methylimidazolium tetrafluoroborate [EMIM][BF$_4$]) have the potential to mitigate the thermal hazards associated with LIBs while avoiding the use of low performance systems or destructive safety measures. Because the hypothesized mechanism for thermal control is based on the thermally activated phase transition, we do not expect similar behavior in mixtures comprising PEO with anions such as PF$_6$ and TFSI, where a thermal phase transition is not observed.[39]

In this article, we describe the use of IL-doped polymer electrolytes as responsive electrolytes that provides thermal and chemical stability at normal operating temperatures, and then impede ion-transport and charge transfer at elevated temperatures where thermal instabilities arise in traditional electrolytes (battery separators traditionally melt between 135 ºC and 170 ºC and ultimately short).[18] This specific responsive polymer electrolyte (RPE), PEO in [EMIM][BF_4], exhibits an inherent temperature based control mechanism that arises from a change in electrolyte conductivity and the composition at electrode/electrolyte interface. These functional materials may permit the incorporation of highly conductivity electrolyte systems in the LIBs needed for high-power, large-format energy storage systems. Previously, we demonstrated the feasibility of using responsive electrolytes in electrochemical systems with copolymers of N-isopropylacrylamide (NIPAM) and (AA) in aqueous systems. [40, 41] These solutions exhibited an order of magnitude decrease in conductivity due to the polymer phase separating above the LCST of the mixture. As a result of the decrease in solution conductivity and ionic strength, we showed that the redox activity and discharge capacity of polyaniline electrodes could be reversibly controlled by changing solution temperature.

While our previous work exemplifies the use of responsive materials to modulate electrochemical processes in aqueous media, these materials are not compatible with Li-ion battery systems that would benefit from high-temperature regulation. However, the knowledge of responsive electrolyte systems was used to design temperature-responsive mixtures that can be used to impede the electrochemical processes in Li-ion electrolytes with increasing temperature. Here, we show 1) how the conductivity of PEO/IL mixtures change with temperature, 2) how lithium salt concentration affects the thermal response and the thermal transition temperature and

3) how Ohmic and charge transfer resistances (at the electrode/electrolyte interface) are affected by temperature in carbon energy storage devices. Further development and applications of PEO/IL electrolytes will provide unique opportunities for battery systems that self-limit their behavior when temperatures become unstable.

2. Results and Discussion

2.1. Thermal Phase Behavior of PEO/[EMIM][BF4]

Based on previous studies of the temperature dependent phase behavior of PEO/[EMIM][BF4] mixtures, we initially studied PEO polymers with two distinct MWs (1.5K and 20K) and two PEO/IL weight compositions (80/20, 50/50). These polymers will be referred to here as PEO/IL (80/20), L-PEO/IL (80/20), PEO/IL (50/50) and L-PEO/IL (50/50), where composition is designated and the low MW (1.5K) PEO mixtures are labeled L-PEO/IL. As demonstrated in **Figure 1**, when the PEO/IL mixtures were heated above their LCST, they separated into a low conductivity PEO-rich phase and a high conductivity IL-rich phase. Below this temperature, the mixture displayed a high conductivity due to the low ionic resistivity of the IL and a favorable PEO/IL conductive pathway. Above the LCST, a liquid-liquid phase separation occurred in the PEO/IL mixture due to increasing entropic contributions to the free energy, [31] consistent with traditional thermally responsive polymers. This separation resulted in a cloudy, opaque solution similar to the solid-liquid phase transition observed in aqueous poly(N-isopropylacrylamide) systems. [42] Driven by density differences between the two materials (~1.3 for [EMIM][BF4] and ~1.0 for PEO), the two liquids gradually separated into a biphasic mixture with time or a further increase in temperature. Due to the high resistivity of PEO in the IL deficient top phase, a drastic decrease in conductivity across the system the biphasic mixture occurred. The change in solution properties and the extent to which the electrochemical behavior of electrochemical systems

change with temperature were measured using the RPEs with simple carbon on stainless steel

mesh electrodes (Figure 1b-c).
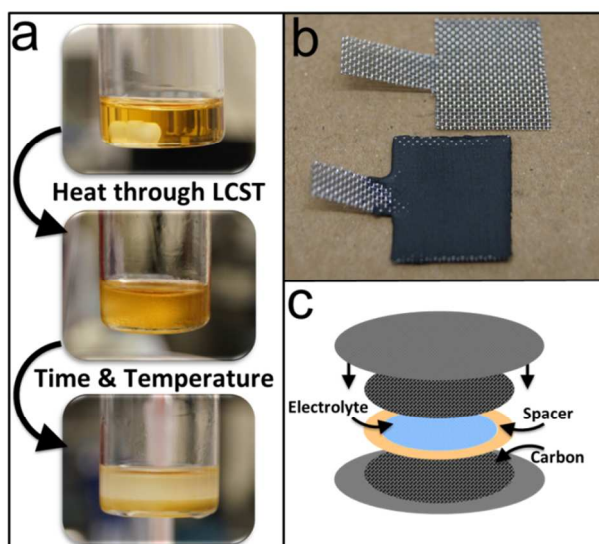
Figure 1. Representations of the RPE phase separation process and electrochemical setup. a) Photographs of the PEO/IL phase separation show that, when heated through the LCST, a cloudy solution forms and eventually turns into a biphasic mixture with time and increased temperature. b) Examples of the carbon coated stainless steel electrodes comprised of either mesoporous (MC, 2000 m^2/g, pore size 13.7 nm) or activated (AC, 150-200 m^2/g, pore size 2.1 nm) carbon materials. c) Schematic of the electrochemical test cell consisting of two carbon electrodes separated by a poly(ether ether ketone) (PEEK) spacer and soaked in the RPE.

Cloud point (CP) measurements were performed in a N_2 purged cell equipped with a temperature

control element in a UV-Vis spectrophotometer to determine the effect of the PEO, IL, and salt

concentration on the phase behavior of the RPE systems. A transmittance of 100% indicated a

well-mixed, single phase solution with a decrease in the transmittance (below 80%) indicated a

thermal phase separation between the PEO and IL. **Figure 2** shows the optical transmission

behavior through the LCST of PEO/IL (80/20) and PEO/IL (50/50) RPEs at a heating rate of 2

ºC/min. Here, we use slightly higher heating rates than conventional CP measurements that aim

for thermodynamically equilibrated LCST values to represent heating rates that may occur in

energy storage devices. All RPE mixtures were well mixed, single phase solutions below 100 ºC.

Solutions containing 20K MW PEO exhibited phase transitions of 118 ℃ and 123 ℃ for the

PEO/IL (80/20) and PEO/IL (50/50), respectively, which are comparable to data obtained by

Lodge et al. using optical transmittance (120-130 ℃), where a heating rate of 1 ℃/min was

employed.[32] These CP values are slightly lower than those obtained by Wu et al. using

differential scanning calorimetry (DSC) measurements (126 ℃ and 128 ℃, respectively) for

mixtures of a similar MW PEO with heating rates up to 20 ℃/min.[35] Their DSC measurements

indicated that the measured LCST increased by only 6.5 ℃ when using heating rates between 10

and 40 ℃/min. A change in optical transmission was not observed in the 1.5K MW PEO

mixtures within our setup, even for temperatures up to 190 ℃. These mixtures, however, showed

visual cloud points of 188 ℃ and 174 ℃ for L-PEO/IL (80/20) L-PEO/IL (50/50), respectively,

which were higher than reported values for 2K MW PEO (160-170 ℃) [32], The increase in the

LCST, however, is expected due to the lower MW PEO used here.
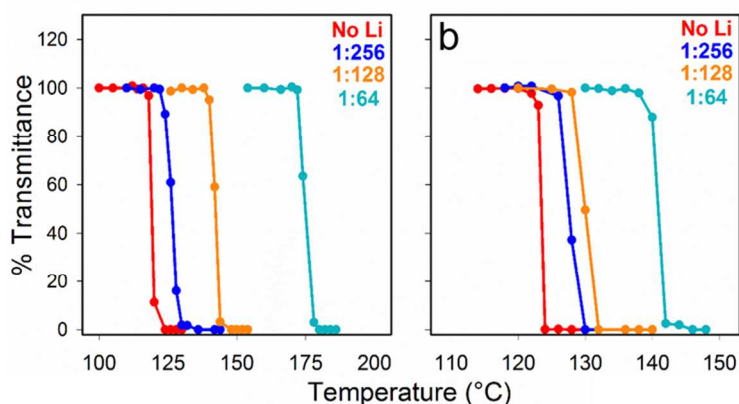
Figure 2. Temperature dependence of optical transmittance for the RPEs. a) Cloud point measurements of mixtures of the PEO/IL (80/20) electrolyte and $LiBF_4$ with Li:O ratios up to 1:64. Cloud points were not observed in Li:O ratios of 1:16 and above. b) Cloud point measurements of mixtures of the PEO/IL (50/50) electrolyte and LiBF4 in Li:O ratios up to 1:64. Cloud points were not observed in Li:O ratios of 1:16 and above. Cloud points or the LCST of each RPE were taken as the point where transmittance reached 80 % of its initial value.

The addition of lithium tetrafluoroborate (LiBF4) to 20K MW PEO/IL (80/20) and PEO/IL

(50/50) mixtures causes an increase in the LCST, which is widely referred to as a salting in effect

in aqueous systems. Figure 2a shows that the addition of $LiBF_4$ in Li:O (# of Li^+ relative to O in

PEO) ratios of 1:256, 1:128, and 1:64 to PEO/IL (80/20) mixtures results in an increase in CP

from 118 ºC (no salt) to 125 ºC, 141 ºC, and 173 ºC, respectively. At high concentrations (Li:O

ratios of 1:16 and above), the LCST of PEO/IL (80/20) disappeared. The temperature range was

maintained below 200 ºC, where PEO degradation occurs. Figure 2b shows that the addition of

the salt has a less pronounced effect on the LCST in the PEO/IL (50/50). The addition of $LiBF_4$

increases the CP from 123 ºC (no salt) to 127 ºC, 129 ºC, and 140 ºC for the 1:256, 1:128, and

1:64 Li:O ratios. The lower influence of salt concentration on the LCST for PEO/IL (50/50) is

attributed to the lower molarity of Li^+ within these solutions, due to a lower composition of PEO

(and therefore O groups) relative to the 80/20 mixture. Similar to PEO/IL (80/20), high salt

concentration mixtures (ratios of 1:16 and above) did not display LCST behavior. Cloud point

measurements for the 1.5K MW PEO with the lithium salt were not measured due to the high

LCST temperatures observed for the L-PEO/IL (80/20) and L-PEO/IL (50/50) and the

degradation point of PEO (approximately 190 ºC - 200 ºC). These results indicate a strong

correlation between phase separation temperature and the composition of each component, but

more importantly, that the LCST can be tailored to achieve a target transition temperature. It

should be noted that the liquid-liquid phase separation between PEO and IL is a reversible

process; that is, as the temperature decreases below the LCST, the mixture returns to the initial

single phase mixture.

2.2. PEO/[EMIM][BF4] Conductivity Change with Temperature

Electrochemical impedance spectroscopy (EIS) measurements were performed in a test cell with stainless steel electrodes and a poly(ether ether ketone)(PEEK) spacer to determine how temperature and phase separation affect the RPE conductivity. Ionic conductivity was determined from the corresponding resistive component of the impedance spectrum using a cell constant calibrated from a 1M NaCl solution at 25 ºC. **Figure 3a** shows the measured conductivity of the salt free RPE systems as a function of temperature, composition, and PEO MW. For both the PEO/IL (80/20) and PEO/IL (50/50) systems, the conductivity rises slowly with temperature, similar to traditional aqueous and nonaqueous electrolytes. Above the LCST, a liquid-liquid phase separation occurs, resulting in PEO-IL phase separation and a decrease in conductivity. As the temperature is further increased, nearly an order of magnitude reduction in conductivity is observed as the electrolyte segregates into the biphasic mixture (PEO-rich top, IL-rich bottom). Unlike the high MW mixtures, the L-PEO/IL (80/20) and L-PEO/IL (50/50) systems exhibited a continual increase in conductivity over the entire range of temperatures, similar to conventional electrolytes. These observations suggest that the very low MW polymer mixtures do not aggregate and coalesce into a biphasic mixture upon phase separation – even though visual changes are observed – which is necessary to inhibit ion-transport through the electrolyte.
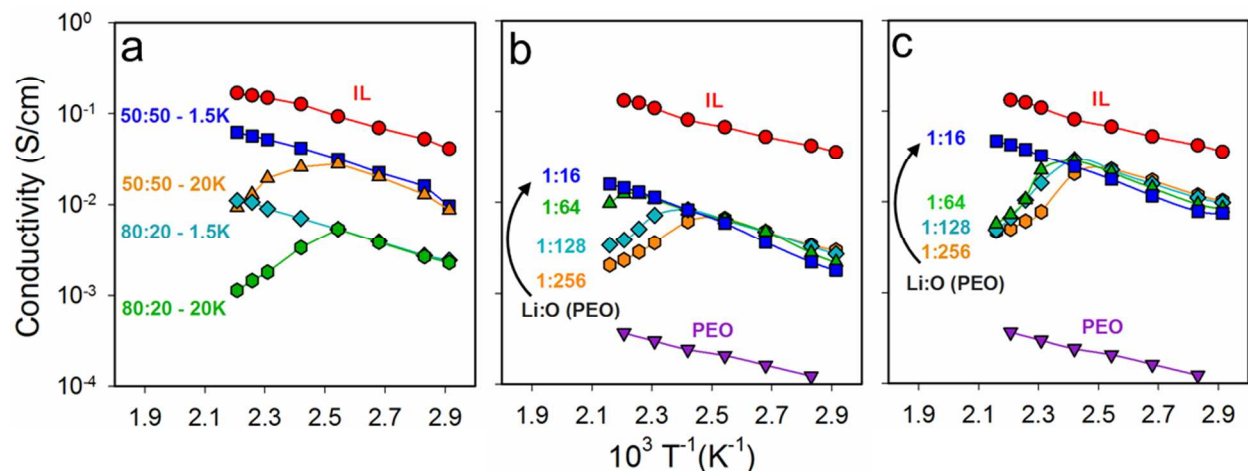
Figure 3. Temperature dependence of ionic conductivity for the RPEs. a) Effect of temperature on the conductivity of the pure IL, [EMIM][BF$_4$] and 1.5K and 20K MW PEO/IL (80/20) and PEO/IL (50/50) mixtures. b) The effect of LiBF$_4$ concentration on the temperature-dependent conductivity of the 20K MW PEO/IL (80/20) system. c) The effect of LiBF$_4$ concentration on the temperature-dependent conductivity of the 20K MW PEO/IL (50/50) system. Concentrations up to 1:64 Li:O are shown to increase the temperature at which conductivity change is observed. For reference, a pure PEO electrolyte with a 1:256 Li:O ratio and a pure IL electrolyte with the same weight percent LiBF$_4$ are shown.

The effect of adding LiBF$_4$ to the PEO/IL (80/20) solutions is shown in Figure 3b for Li:O ratios of 1:256, 1:128, 1:64, and 1:16. As the salt concentration is increased, the temperature at which the conductivity begins to decrease also increases, consistent with the CP measurements described above. At high concentrations (Li:O ratios of 1:16 and above), no change in conductivity was observed, as these compositions did not exhibit an LCST phase transition. Figure 3c shows that increasing the LiBF$_4$ concentration in PEO/IL (50/50) solutions resulted in an increase in the temperature at which conductivity changed. The shift in temperature is much less in PEO/IL (50/50) compared to PEO/IL (80/20), which is consistent with the CP measurements above and attributed to lower Li$^+$ concentrations. Unlike traditional PEO-LiBF$_4$ and IL-LIBF$_4$ electrolytes, these RPE systems show an abrupt decrease in conductivity near their LCST, except for high Li$^+$ concentrations. As seen with CP measurements, lithium salt concentration (along with composition and MW) can be used to tailor the temperature at which

the phase transition occurs and causes ion-transport to become inhibited. While the bulk electrolyte exhibits a reversible phase transition, this process was slow and required the solution to remain above its melting point (~70 °C) for many days. However, we did not observe reversibility in the electrolyte conductivity when the electrolyte is confined in the electrochemical cells with carbon or stainless steel electrodes, even after 1 week.

2.3. Electrochemical Characterization

The utilization of RPE solutions in an energy storage cell was investigated using carbon coated stainless steel mesh electrodes. An symmetric 2-electrode cell was fabricated using carbon electrodes soaked in the RPEs overnight separated by a PEEK washer/spacer. Two types of carbons were investigated: mesoporous carbon (MC) with a low surface area and large pore diameter (50-100 m^2/g, 13.7 nm) and activated carbon (AC) with a large surface area and small pore diameter (2000 m^2/g, 2.1 nm). The mechanism for energy storage within these electrodes is electrical double layer capacitance, where ions physically accumulate at the electrode/electrolyte interface in a non-Faradaic process (no charge transfer). Very high surface area carbons (AC) can achieve much higher capacitance values compared to lower surface area materials with open porous structures (MC), but are limited by lower discharge rates and power density due to the tortuous ion transport pathways. Due to the high viscosity of the PEO/IL (80/20) mixtures, which greatly limits ion transport and adsorption, electrochemical measurements on porous carbon were only performed using PEO/IL (50/50) electrolytes.

Cyclic voltammetry (CV) was used to measure the electrical double layer capacitance of cells with PEO/IL electrolytes, which depends on accessible surface area and ion concentration.

Figure 4 shows CV profiles of symmetric supercapacitors containing AC and MC carbon

electrodes in pure IL and two of the RPEs of interest over a range of temperature from 100 ºC up

to 160 ºC. Devices comprising AC electrodes in pure IL exhibit a monotonic increase current

with temperature, as expected, due to the increase in conductivity (Figure 4a). The integrated

area under the profiles, which is a representation of the amount of charge stored, correspondingly

increases with temperature, as shown in inset of Figure 4a (charge values are normalized to the

initial value at 100 ºC). CV profiles of cells comprising AC electrodes in L-PEO/IL (50/50)

electrolyte are shown in Figure 4b for the system heated from 100 ºC to 160 ºC. Similar to the

pure IL, the relative amount of charge stored in these electrodes initially increases between 100

ºC and 120 ºC, consistent with an increase in ion conductivity. Although the L-PEO/IL (50/50)

did not display a change in conductivity or a visual CP until above 174 ºC, the current measured

during CV cycling decreased as the cell was heated about 120 ºC. This observation was initially

surprising as the conductivity of these electrolytes was shown to continuously increase with

temperature (Fig. 3a). However, Wu et al demonstrated that a thermal transition occurs in low

MW PEO/IL systems between 120 and 130 ºC utilizing DSC.[35] The decrease in current mesaured

in cells above 140 ºC supports our hypothesis that the L-PEO/IL (50/50) electrolytes do in fact

exhibit a thermally activated phase separation that cannot be detected cloud point measurements,

in which PEO aggregates in solution and within the electrode pores and then adsorbs to the

carbon. Interestingly, the rectangular shape of the CV profile indicates that ion diffusion is not a

limiting factor and that either a loss of electrode area has occurred or in increase in resistance for

charges entering the double layer has increased. From these observations, we can deduce that a

PEO rich phase or coating is formed inside the nanopores of AC creating a barrier to charge

insertion and accumulation at the electrode/electrolyte interface. The inset in Figure 4b shows

that the capacitance at 160 ℃ decreases to approximately 70% of if its initial value at 100 ℃ (or

50% of the capacitance at 120 ℃). To put this value in perspective, devices utilizing IL

electrolyte exhibited a nearly 2x increase in capacitance, which shows that the L-PEO/IL

electrolyte is effective in impeding electrochemical processes at elevated temperature (even

though conductivity still increases).
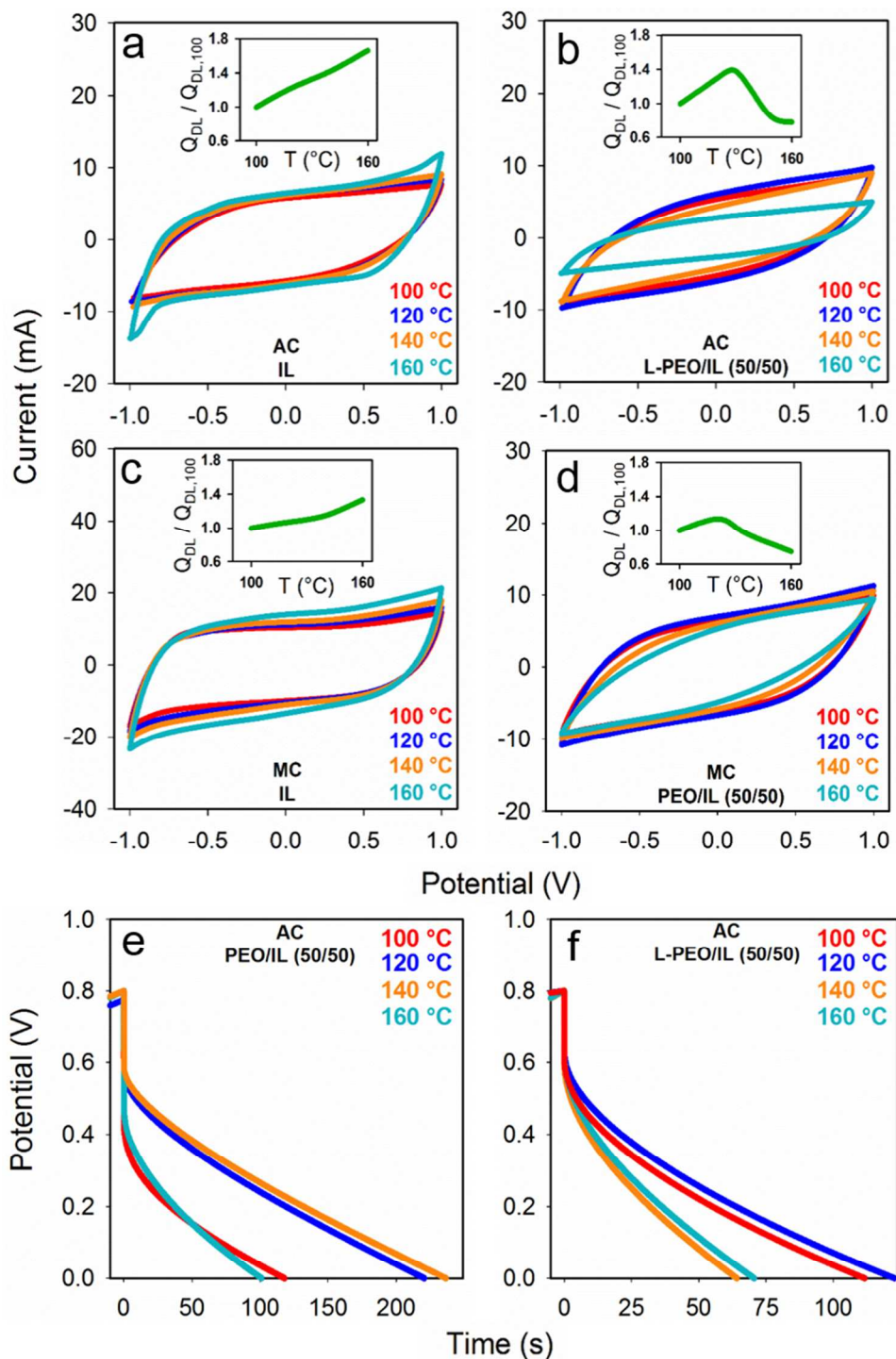
Figure 4. Temperature dependence of CV profiles for selected RPEs (100-160 ºC). a) CV profiles at a scan rate of 5 mV/s for AC electrodes and pure IL electrolytes. b) CV profiles for AC electrodes and L-PEO/IL (50/50). c) CV profiles at 300 mV/s using MC electrodes and the pure IL electrolyte. d) CV profiles for the MC electrodes using the PEO/IL (50/50). e) Constant current discharge profiles for AC electrodes in the L-PEO/IL (50/50). f) Constant current discharge profiles for AC electrodes in the PEO/IL (50/50) electrolyte. Insets in (a-d) show the

change in capacitance (integrated area under CV profiles) at each temperature and are normalized to the initial value at 100 ºC.

Comparable to devices comprising AC electrodes in pure IL, cells containing MC electrodes in pure IL exhibit a linear increase in capacitance with temperature over the range of 100 ºC to 160 ºC, as shown in Figure 4c. The EDLC of devices using PEO/IL (50/50) electrolyte also increases initially until the cell reaches the LCST of 123 ºC. Above this temperature, however, the EDLC decreases as a result of the lower conductivity (Fig. 3a) and the formation of a barrier to charging the electrode/electrolyte interface. Contrary to L-PEO/IL (50/50) devices that exhibit a decrease in double layer capacitance, these devices also exhibit a noticeable change in the CV profile shape (rectangular to egg-shaped) which is indicative of ion diffusion limitations. The inset in Figure 4d shows that the capacitance above 160 ºC again decreases to approximately 70% of if its value at 100 ºC.

Constant current charge-discharge measurements were performed on the AC electrodes in both the PEO/IL (50/50) and L-PEO/IL (50/50) electroltyes, with the discharge profiles shown in Figures 4e-f. The applied current was set for each system such that the discharge time was approximately 110 seconds at 100 ºC. We found that the discharge capacity for cells utilizing the high molecular weight PEO/IL electrolyte increased up to 140 ºC as the solution conductivity increases. Above this temperature, the PEO-IL mixture phase separates and a rapid decrease in discharge capacity (total discharge time) was observed. The decrease in conductivity above the LCST results in an increase in solution resistance and an increase in ohmic drop (initial change in voltage upon switching the current polarity from charging to discharging, $t = 0$), as shown in Fig. 4e. Similarly, the discharge capacity for devices comprising the low molecular PEO/IL

electrolyte decreases above 140 ºC; however, this system did not exhibit a corresponding

decrease in conductivity. As a result, a nearly temperature-indepedent ohmic drop was observed,

as shown in Figure 4f, suggesting that the solution conductivity alone cannot account for the

decrease in discharge capacity. Accordingly, the polymer-IL phase separation must result in

additional resistances at the electrode/electrolyte interface, which will be identified below using

impedance analysis.

Electrochemical impedance spectroscopy (EIS) measurements were performed to determine the

mechanism for the decrease in electrochemical activity on AC and MC electrodes above the

LCST of the electrolyte. Understanding the mechanism of ion adsorption and charge transfer

inhibition is critical for further developing electrolyte materials and compositions that can be

used to inhibit electrochemical processes in devices that tend of overheat and exhibit thermal

runaway, such as Li-ion batteries. Measurements were carried out using symmetric cells of each

electrode type in pure IL electrolytes and all four RPEs, as shown in **Figure 5**. While CV

measurements reveal changes in ELDC properties for a specific scan rate, EIS provides insight

into electrochemical processes over a range of time-scales, which can be fit to extract resistive

and capacitive components. Carbon EDLCs are often modeled using de Levie's Transmission

Line Model (TLM) equivalent circuit due to their highly porous and tortuous structure and

intricate internal resistance. Here, we use a more simplified EIS model to reveal two important

electrode/electrolyte characteristics: the Ohmic resistance (R_S), which is the intersection point

with the x-axis in the high frequency region, and the internal resistance to charging the EDLC

electrode/electrolyte interface or the "double layer" resistance.[43] This internal resistance was

determined with the use of the EIS data fitting program ZVIEW and applying a modified

Randles circuit model (charge transfer and Warburg impedance in parallel to a constant phase

element) of the high- to mid-range frequency region. The in-series combination of the pseudo

charge transfer resistance and Warburg impedance is referred to here as the "double layer"

resistance (R_{DL}). The pseudo charge transfer resistance results from a combination of ion

mobility (solution conductivity) in the nanostructured carbon pores and the PEO physisorption

on at the electrode/electrolyte interface.[44, 45]
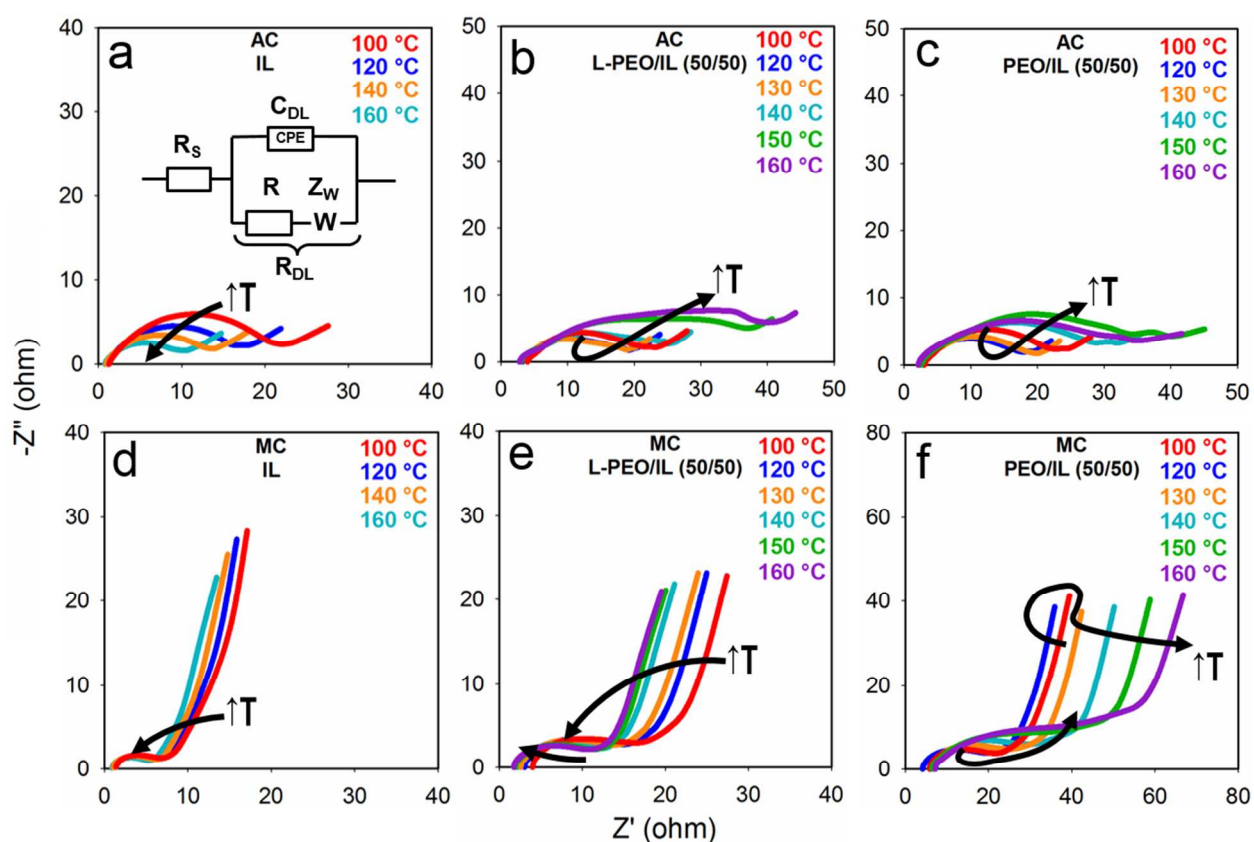
Figure 5. Temperature dependence of electrochemical impedance spectroscopy measurements for the RPEs. a) Nyquist plot for the pure IL, [EMIM][BF$_4$], on the AC electrodes with the modified Randles circuit. b) L-PEO/IL (50/50) on AC electrodes. c) PEO/IL (50/50) on AC electrodes. d) IL on MC electrodes. e) PEO/IL (50/50) on MC electrodes. f) The PEO/IL (50/50) on MC electrodes. All measurements were performed at a potential of 1 V over the frequency range of 0.1 Hz – 1 MHz, with an amplitude of 20 mV, and over the temperature range 100-160 °C. Arrows indicate the evolution of the Nyquist plots with temperature.

For the IL, L-PEO/IL (50/50) and PEO/IL (50/50) electrolytes on AC electrodes (Figures 5a-c),

EIS measurements reveal a relatively high internal "double layer" resistance (R_{DL}) that arises

from impeded ion transport within the nanoscale pores of the AC. The Nyquist plots indicate that devices comprising each electrolyte are highly dependent on this internal resistance over the range of frequencies down to 1 Hz, where characteristics of diffusion limited behavior are observed (45° slope in $-Z''$ vs Z'). In Figure 5a, devices containing pure IL exhibit a R_{DL} that decreases with increasing temperature due increasing ion conductivity, similar to conventional electrolyte solutions. Devices with AC electrodes in L-PEO/IL (5050) initially show a decrease in R_{DL} with increasing temperature (below the LCST) as evidenced by the slight decrease in high- to mid-range frequency semicircle radius (Figure 5b). Even though we observed that the solution conductivity continues to increase above the LCST (Figure 3a), from the EIS measurements, we found that semicircle radius of the Nyquist plot associated with R_{DL} increases drastically, indicating an increase in double layer resistance. The increased resistance is attributed to an increased PEO concentration within the pores of the electrodes combined with polymer physisorption on the carbon surface, which supports our observations of decreased electrode capacitance. Figure 5c shows that devices containing PEO/IL (50/50) display a similar but less significant trend. Although devices with the 20k MW PEO electrolyte experience a decrease in conductivity with increasing temperature, these polymers are larger than the AC pores, thereby preventing the polymer from coating the pore walls above the LCST. Without complete coverage or physisoprtion on the carbon surface (as observed with 1.5K MW PEO), the electrolyte containing 20K MW PEO has a limited impact on the double layer resistance in the nanoporous electrodes. Interestingly, these results confirm that electrochemical activity is more strongly affected by polymer adsorption on the electrode interface than a decrease in ion conductivity above the phase transition temperature (LCST).

In devices comprising MC electrodes with IL, L-PEO/IL (50/50) and PEO/IL (50/50) electrolytes (Figures 5d-f), EIS analysis reveals a much lower R_{DL} (smaller hemisphere radius) as a result of the larger pore size and ion accessibility in the mesoporous carbon. Unlike in devices prepared with the AC electrodes, the limiting charging/discharging mechanism changes from R_{DL} to ion diffusion at much higher frequencies, 10-20 Hz, indicating that cells with MC electrodes will be limited by ion mobility (conductivity) under most operating conditions. In such systems, we expect electrolyte conductivity to have a more significant influence on the electrochemical activity. As expected, R_{DL} decreases with increasing temperature in devices with pure IL electrolytes (Figure 5d), which is similar to the behavior on AC electrodes. Since the mechanism on MC electrodes is governed by ion-transport rather than polymer adsorption, we don't a significant change in R_{DL} above the LCST of L-PEO/IL (50/50), as shown in Figure 5e. In fact, the characteristics of the Nyquist plot are quite similar to results from devices with pure IL, as both electrolytes exhibit a continuous increase in conductivity with increasing temperature. The radius of the high- to mid-range frequency semicircle continues to decrease at temperatures up to 160 °C, indicating a decrease in the R_{DL}. Contrary to the behavior in devices with AC electrodes, electrolytes using low MW PEO do not seem effect to significantly affect the resistance of cells comprising carbon electrodes with large pores (> 13 nm). Above we showed that electrolytes comprising high MW PEO display a change in conductivity about their LCST. As the ion-adsorption mechanism of MC electrodes is governed by ion-diffusion it is expected that the electrochemical behavior of MC devices with the PEO/IL (50/50) electrolyte correlate with the conductivity measurements of these systems (Figure 3c). Indeed, these cells initially show an initial decrease in R_{DL} as the temperature increases, followed by a significant increase in capacitance, as evidenced by the increasing radius of the Nyquist semicircle (Figure 5f) above

120 ºC. In carbon electrodes with large pores, electrochemical activity can be modulating using high MW PEO by inhibiting ion transport between the electrodes.

A summary of the changes for both the Ohmic resistance and double layer resistance over the temperature range of 100-160 ºC is shown in **Figure 6**. Values for resistances at each temperature were modeled with a modified Randles circuit and normalized to the resistance at 100 ºC to display each profile on the same plot. Figure 6a shows how the Ohmic resistance (series) in the AC electrodes changed when using the pure IL, L-PEO/IL (50/50), and PEO/IL (50/50) electrolytes. As previously described, the solution resistance (which is a large component of the Ohmic resistance in the electrochemical cell) only increases the 20K MW PEO electrolyte, which exhibits a decrease in conductivity above the LCST. With the MC electrodes (Figure 6b), a similar but more pronounced change in the Ohmic resistance is observed since the governing mechanism in these materials is ion-diffusion (under the test conditions).
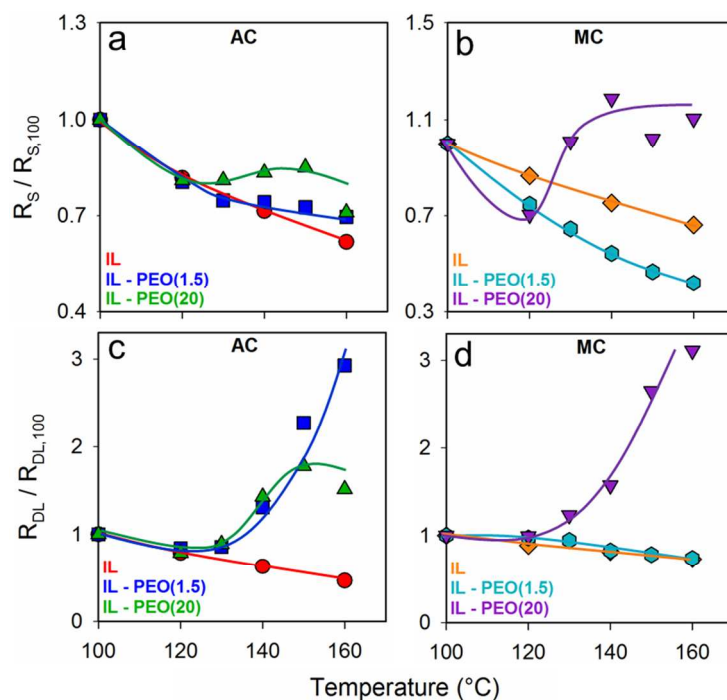
Figure 6. Temperature dependence of the Ohmic and double layer resistances of the AC and MC electrodes with the RPEs. a) Normalized Ohmic resistance, R_S, of the IL, L-PEO/IL (50/50), and PEO/IL (50/50) on the AC electrodes. b) Similar normalized Ohmic resistance on MC electrodes. c) Normalized double layer resistance, R_{DL}, of the IL and 50:50 PEO:IL RPEs on the AC electrodes. d) Similar normalized double layer resistance on MC electrodes. All resistance values were normalized to values at 100 °C. Trend lines are drawn for reference.

The double layer resistance in the AC electrodes is strongly affected by the phase transition of L-PEO/IL (50/50) and PEO/IL (50/50) electrolytes above their LCST (Figure 6c). As expected, devices with pure IL electrolyte show a decrease in R_{DL} as the temperature increases. Both the L-PEO/IL (50/50) and PEO/IL (50/50) electrolytes show a drastic increase in R_{DL} when heated above their LCST. A more pronounced increase is seen in the AC electrodes with the L-PEO/IL (50/50), since the smaller PEO chains can infiltrate the nanoscale (2 nm) pores and absorb on the electrode surface. On the MC electrodes, the double layer resistance increases for devices with pure IL and L-PEO/IL (50/50), as both systems exhibit and increase in conductivity with increasing temperature (Figure 6d). Cells with PEO/IL (50/50) electrolytes, however, show a 3-fold increase in R_{DL} above the LCST, as expected due to the decrease in ion conductivity between the carbon electrodes, which reduces ion concentrations near the electrode surface. The charge-discharge and cyclic voltammetry measurements presented in Figure 4 suggest that a temperature lag exists between the phase separation and the change in electrochemical performance. This liqui-liquid phase transition is a kinetically limited process and requires time for the polymers to phase separate and coalesce into a new phase. Even though more than 30 min were allowed for the cells to equilibrate at each temperature, it is feasible that the systems were not in fact at equilibrium. However, the normalized ohmic and charge transfer resistances presented in Figure 6 indicate that these resistances actually begin to increase almost exactly at the LCST measured above for each respective system (120-130 °C). As the temperature further

increases above the LCST, the tendency for materials to aggregate increases, which leads to further increases in these resistance values, as shown by the impedence measurements.

3. Conclusion

In summary, we have shown how a LCST phase transition can be used to modulate the electrochemical activity of electrode interfaces, which can be used to control the function of energy storage devices. Using electrolytes comprised of an ionic liquid, [EMIM][BF$_4$] and PEO, and Li$^+$ salts, we showed that the solution conductivity can be designed to decrease when the temperature of the system increasing beyond the LCST of the mixture. Upon phase separation of PEO from the IL, the double layer resistance of carbon electrodes increases as a result of either polymer adsorption on the electrode interface (low MW PEO in 2 nm pores), or a decrease in conductivity which limits the ion concentration near the electrode surface (high MW PEO in >13 nm pores). Furthermore, we demonstrate how the composition of PEO and IL, in addition to the concentration of Li$^+$ salt affect the temperature at which the transition occurs and the extent to which the conductivity can be decreased. These polymer systems show promise for future electrolytes as they are capable of altering both the Ohmic (solution) resistance and the double layer capacitance of carbon based devices. Our electrolyte design provides a novel approach to mitigating thermal hazards associated with batteries and electrochemical devices overheating, and further development of similar responsive electrolytes will inevitability have a tremendous impact on Li-ion batteries.

4. Experimental Section

Electrolyte Preparation: Polymer electrolyte solutions were prepared by mixing PEO (1,500 MW (Fluka), 20,000 MW (Polysciences)), ([EMIM][BF$_4$]) (Ionic Liquid Technologies, 98+%),

and LiBF$_4$ (Sigma Aldrich) while stirring at 90ºC under N$_2$ for 30 minutes. Once mixed, solutions were dried under vacuum (mTorr) at 90ºC while stirring for at least 12 hours, then immediately transferred and sealed in the electrochemical or spectroscopic test cells.

Cloud Point Measurement: The cloud point of the PEO/[EMIM][BF4]/LiBF4 solutions was determined using optical transmittance. Electrolyte solutions were mixed and dried under vacuum (mTorr) at 90ºC while stirring for 12 hours then purged with N$_2$ prior to transmission measurements. Temperature-controlled cells with sapphire windows were placed in a UV-Vis spectrophotometer (Varian Cary 50 Bio) and heated at a rate of 2 °C/min while continually recording UV-Vis scans. An average transmittance was calculated over a range of wavelengths (600-800 nm). The cloud point or LCST was defined as the temperature at which the transmittance dropped below 80% of its initial value.

Electrode Preparation: Carbon electrodes were prepared using a mesoporous carbon (Sigma Aldrich, surface area ~50-100 m^2/g, average pore diameter 13.7 nm) and an activated carbon (MTI, surface area 2000 m^2/g, average pore size 2.1 nm). Electrodes were prepared by dispersing the mesoporous (MC) or activated carbon (AC), conductive graphite (MTI), and poly(vinylidene fluoride) (Sigma Aldrich) in an 80/10/10 weight percent ratio in N-methyl-2-pyrrolidone (Acros). The resulting carbon pastes were then spread on 316 stainless steel sheets (60 x 60 mesh, roughly 20mm x 20mm squares each). Electrodes were dried for at least 12 hours at 100ºC under vacuum and then soaked in their respective electrolyte (PEO-IL mixture) for at least 6 hours at 100ºC under vacuum (~30 in Hg) prior to electrochemical testing.

Electrochemical Characterization: Electrochemical measurements were performed with a Gamry galvonstat/potentiostat in a 2-electrode setup using a split test coin cell (MTI, EQ-STC) mounted in a modified convection oven. Solutions were heated at approximately 2 ºC/min and allowed to equilibrate at set temperatures for 30 minutes prior to electrochemical measurements. Bulk conductivity measurements were conducted on electrolytes between stainless steel electrodes separated by a 1mm thick poly(ether ether ketone) (PEEK) spacer with an internal diameter of 12 mm over a temperature range of 70 to 180 ºC. Electrochemical impedance spectroscopy (EIS) was performed over a frequency range of 1 Hz to 1 MHz (0V, 20 mV RMS). Ionic conductivity was determined from the corresponding resistive component of the impedance spectrum and calculated using a cell constant calibrated from a 1M NaCl solution at 25 ºC. Two electrode cells were constructed with either MC or AC electrodes, which were separated by a PEEK spacer (t = 1 mm, ID = 12mm) and the PEO-IL electrolyte. Cells were characterized using cyclic voltammetry (CV), constant current charge-discharge (XD) and EIS for the pure IL and PEO-IL electrolytes over a temperature range of 100 to 180 ºC. CV scans were performed at 300 mV/s (MC) and 5 mV/s (AC) over a potential range of -1.0 to 1.0 V. XD was performed on the AC electrodes at currents of 3.2 mA, for the L-PEO/IL (50/50), and 2.0 mA, for the PEO/IL (50/50), over a potential range of 0.0 to 0.8V. EIS analysis was performed over a frequency range of 100 mHz to 1 MHz (1V, 20 mV RMS).

Acknowledgements

Author Contributions

MER and JCK designed and planned the experiments and wrote the manuscript. JCK and RG prepared the polymer electrolytes and performed the electrochemical analysis.

Competing Financial Interests

References

[1]   J. Ding, D. Zhou, G. Spinks, G. Wallace, S. Forsyth, M. Forsyth, D. MacFarlane, *Chem. Mater.* **2003**, 15, 2392-2398.

[2]   W. Lu, A. G. Fadeev, B. Qi, E. Smela, B. R. Mattes, J. Ding, G. M. Spinks, J. Mazurkiewicz, D. Zhou, G. G. Wallace, D. R. MacFarlane, S. A. Forsyth, M. Forsyth, *Science* **2002**, 297, 983-987.

[3]   D. Kuang, S. Uchida, R. Humphry-Baker, S. M. Zakeeruddin, M. Grätzel, *Angew. Chem. Int. Ed.* **2008**, 47, 1923-1927.

[4]   G. T. Kim, S. S. Jeong, M. Z. Xue, A. Balducci, M. Winter, S. Passerini, F. Alessandrini, G. B. Appetecchi, *J. Power Sources* **2012**, 199, 239-246.

[5]   B. Garcia, S. Lavallée, G. Perron, C. Michot, M. Armand, *Electrochim. Acta* **2004**, 49, 4583-4588.

[6]   H. Nakagawa, S. Izuchi, K. Kuwana, T. Nukuda, Y. Aihara, *J. Electrochem. Soc.* **2003**, 150, A695-A700.

[7]   S. Seki, Y. Ohno, Y. Kobayashi, H. Miyashiro, A. Usami, Y. Mita, H. Tokuda, M. Watanabe, K. Hayamizu, S. Tsuzuki, *J. Electrochem. Soc.* **2007**, 154, A173-A177.

[8]   M. Armand, F. Endres, D. R. MacFarlane, H. Ohno, B. Scrosati, *Nat. Mater.* **2009**, 8, 621-629.

[9]   T. E. Sutto, T. T. Duncan, T. C. Wong, K. McGrady, *Electrochim. Acta* **2011**, 56, 3375-3379.

[10]   J. B. Goodenough, Y. Kim, *Chem. Mater.* **2009**, 22, 587-603.

[11]   A. Lewandowski, A. Świderska-Mocek, *J. Power Sources* **2009**, 194, 601-609.

[12]   T. Welton, *Chem. Rev.* **1999**, 99, 2071-2084.

[13]   G.-H. Kim, A. Pesaran, R. Spotnitz, *J. Power Sources* **2007**, 170, 476-489.

[14]   P. G. Balakrishnan, R. Ramesh, T. Prem Kumar, *J. Power Sources* **2006**, 155, 401-414.

[15]   E. P. Roth, C. J. Orendorff, *Electrochem. Soc. Interface* **2012**, 21, 45-49.

[16]   W. H. Meyer, *Adv. Mater.* **1998**, 10, 439-448.

[17]   A. Manuel Stephan, *Eur. Polym. J.* **2006**, 42, 21-42.

[18]   C. J. Orendorff, *Electrochem. Soc. Interface* **2012**, 21, 61-65.

[19]   P. Arora, Z. Zhang, *Chem. Rev.* **2004**, 104, 4419-4462.

[20]   J. W. Fergus, *J. Power Sources* **2010**, 195, 4554-4569.

[21]   X. Huang, *J. Solid State Electr* **2011**, 15, 649-662.

[22]   Y.-S. Ye, J. Rick, B.-J. Hwang, *J. Mater. Chem. A* **2013**, 1, 2719-2743.

[23]   J.-H. Shin, W. A. Henderson, S. Passerini, *Electrochem. Commun.* **2003**, 5, 1016-1020.

[24]   Y. Kumar, S. A. Hashmi, G. P. Pandey, *Solid State Ionics* **2011**, 201, 73-80.

[25]   T. Y. Kim, H. W. Lee, M. Stoller, D. R. Dreyer, C. W. Bielawski, R. S. Ruoff, K. S. Suh, *ACS Nano* **2010**, 5, 436-442.

[26]   J. Yuan, D. Mecerreyes and M. Antonietti, *Prog. Polym. Sci.* **2013**, 38, 1009-1036.

[27]   H. Hu, W. Yuan, Z. Jia and G. L. Baker, *RSC Adv.* **2015**, 5, 3135-3140.

[28]   H. Hu, W. Yuan, L. Lu, H. Zhao, Z. Jia, G. L. Baker, *J. Polym. Sci. A1* **2014**, 52, 2104-2110.

[29]   S. Seki, N. Serizawa, K. Takei, K. Dokko, M. Watanabe, *J. Power Sources* **2013**, 243, 323-327.

[30]   H. Moon, R. Tatara, T. Mandai, K. Ueno, K. Yoshida, N. Tachikawa, T. Yasuda, K. Dokko, M. Watanabe, *J. Phys. Chem. C* **2014**, 118, 20246-20256.

[31]   H.-N. Lee, T. P. Lodge, *J. Phys. Chem. Lett.* **2010**, 1, 1962-1966.

[32]   H.-N. Lee, N. Newell, Z. Bai, T. P. Lodge, *Macromolecules* **2012**, 45, 3627-3633.

[33]   R. Tsuda, K. Kodama, T. Ueki, H. Kokubo, S.-i. Imabayashi, M. Watanabe, *Chem. Commun.* **2008**, 4939-4941.

[34]   R. P. White, J. E. Lipson, *Macromolecules* **2013**, 46, 5714-5723.

[35]   W. Li, P. Wu, *Soft Matter* **2013**, 9, 11585-11597.

[36]   F. Liu, M. W. Urban, *Prog. Polym. Sci.* **2010**, 35, 3-23.

[37]   M. A. C. Stuart, W. T. Huck, J. Genzer, M. Müller, C. Ober, M. Stamm, G. B. Sukhorukov, I. Szleifer, V. V. Tsukruk, M. Urban, *Nat. Mater.* **2010**, 9, 101-113.

[38]   P. T. Mather, *Nat. Mater.* **2007**, 6, 93-94.

[39]   T. Ueki, Polym. J. **2014**, 46, 646-655.

[40]   J. C. Kelly, M. Pepin, D. L. Huber, B. C. Bunker, M. E. Roberts, *Adv. Mater.* **2012**, 24, 886-889.

[41]   J. C. Kelly, D. L. Huber, A. D. Price, M. E. Roberts, *Under Review* **2014**.

[42]   H. Schild, *Prog. Polym. Sci.* **1992**, 17, 163-249.

[43]   R. De Levie, *Electrochimica Acta* **1963**, 8, 751-780.

[44]   J. Gamby, P. Taberna, P. Simon, J. Fauvarque, M. Chesneau, *J. Power Sources* **2001**, 101, 109-116.

[45]   E. Lust, G. Nurk, A. Jänes, M. Arulepp, P. Nigu, P. Möller, S. Kallip, V. Sammelselg, *J. Solid State Electr* **2003**, 7, 91-105.

Responsive Electrolytes that Inhibit Electrochemical Energy Conversion at Elevated Temperatures

J. C. Kelly, R. Gupta, and M. E. Roberts*

Ionic liquid-doped polymers as used responsive electrolytes to inhibit device operation at the elevated temperatures where thermal hazards exist.